JOURNAL OF MATERIALS SCIENCE 31 (1996) 3541–3547

Preparation and optical properties of transparent glass-ceramics containing $LiGa_5O_8$: Cr^{3+}

I. YAMAGUCHI, K. TANAKA, K. HIRAO, N. SOGA
Division of Material Chemistry, Faculty of Engineering, Kyoto University, Sakyo-ku, Kyoto 606-01, Japan

Transparent glass-ceramics containing $LiGa_5O_8:Cr^{3+}$ crystallites have been prepared by heat treatment of Li_2O–Ga_2O_3–SiO_2–Cr_2O_3 glassy material. Average crystallite size evaluated from the full-width at half-maximum of the X-ray diffraction lines varies from about 3–7 nm as the heat-treatment temperature increases from 650 °C to 800 °C. The ligand field strength of the Cr^{3+} ion estimated from optical absorption measurements increases with an increase in the heat-treatment temperature. The fluorescence spectra of the glass-ceramics resemble that of $LiGa_5O_8:Cr^{3+}$ polycrystal. In particular, for the specimen containing a crystallite of 7 nm, intense emission due to the $^2E \rightarrow {}^4A_2$ transition has been observed. These optical measurements demonstrate that the Cr^{3+} ions are incorporated into $LiGa_5O_8$ microcrystals in the present glass-ceramics. For the transparent glass-ceramics and $LiGa_5O_8:Cr^{3+}$ polycrystal, the temperature dependence of the peak position of the zero-phonon line (*R*-line) has been analysed assuming that the electronic transition is described by the Raman process and the vibrational density of state is expressed by the Debye model. The Debye temperature of the transparent glass-ceramics is slightly lower than that of $LiGa_5O_8:Cr^{3+}$ polycrystal, indicating that the softening of the phonon occurs in the $LiGa_5O_8:Cr^{3+}$ microcrystal precipitated in the transparent glass-ceramics.

1. Introduction

Transparent glass-ceramics doped with transition metal ions are expected to be used as optical materials such as a solid-state lasers and luminescent solar concentrators [1]. Thus far, transparent glass-ceramics containing Cr^{3+}-doped $MgAl_2O_4$, $ZnAl_2O_4$, mullite, β-quartz solid solution and ZrO_2 have been reported [2–9]. Also recently, an attempt was made to prepare transparent glass-ceramics containing $ZnAl_2O_4:Co^{2+}$ and $LiGa_5O_8:Co^{2+}$, and their optical properties were examined [10, 11]. In the $ZnAl_2O_4$-containing glass-ceramics, almost all the Co^{2+} ions are effectively incorporated into the $ZnAl_2O_4$ microcrystalline phase and replace the Zn^{2+} ions in the tetrahedral sites. In contrast, some of the Co^{2+} ions remain in the glass matrix in the transparent $LiGa_5O_8$-containing glass-ceramics. In the Cr^{3+}-containing systems, Cr_2O_3 acts as a nucleating agent. For instance, $MgCr_2O_4$ precipitates initially and converts to $MgAl_2O_4:Cr^{3+}$ during the crystal growth process of $MgAl_2O_4:Cr^{3+}$ from magnesium aluminosilicate glass containing Cr_2O_3 [4]. It is of interest to examine whether the Cr^{3+} ion can be incorporated or not into the $LiGa_5O_8$ crystalline phase in the $LiGa_5O_8$-containing glass-ceramics where all the Co^{2+} ions are not incorporated into the microcrystalline phase. Besides, as the ionic radius of Ga^{3+} is larger than that of Al^{3+}, it is expected that the ligand field strength around Cr^{3+} is smaller in the gallate crystal than in the aluminate crystal, and hence, the optical properties of $LiGa_5O_8:Cr^{3+}$-containing transparent glass-ceramics are different than those of transparent glass-ceramics containing aluminate crystals such as $ZnAl_2O_4$ and $MgAl_2O_4$. In the present investigation, an attempt was made to prepare transparent glass-ceramics containing $LiGa_5O_8:Cr^{3+}$ and to examine optical properties of the resultant specimens.

2. Experimental procedure

2.1. Preparation of specimens

Glass-ceramics were prepared by the heat treatment of as-quenched glassy material with a composition $13Li_2O \cdot 23Ga_2O_3 \cdot 64SiO_2 \cdot 0.1Cr_2O_3$ (molar ratio). Raw materials, Li_2CO_3, Ga_2O_3, SiO_2 and Cr_2O_3, were mixed thoroughly and melted in a platinum crucible at 1600 °C for 2 h in air. The melt was quenched by being pressed with two iron plates; the spacing between which was about 1.5 mm. A great part of the resultant bulk specimen was green and transparent, although a small fraction of the specimen was opaline. Only the transparent part was used for subsequent experiments. Differential thermal analysis (DTA) of the as-quenched specimen, the result of which is shown in Fig. 1, revealed that the glass transition temperature was 635 °C and the crystallization temperatures were 719 and 865 °C. Therefore, the as-quenched specimen was annealed at 635 °C for 15 min. The resultant specimen was polished to about

0022–2461

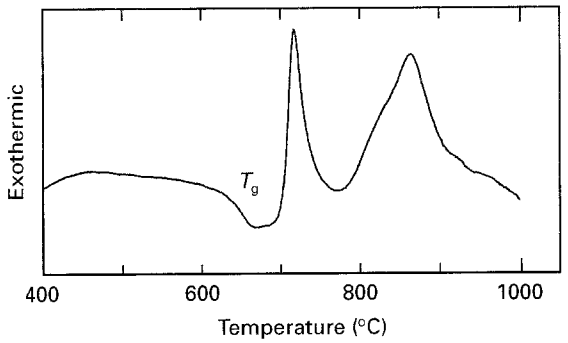

Figure 1 Differential thermal analysis curve of $13Li_2O \cdot 23Ga_2O_3 \cdot 64SiO_2 \cdot 0.1Cr_2O_3$ as-quenched specimen. T_g denotes the glass transition temperature.

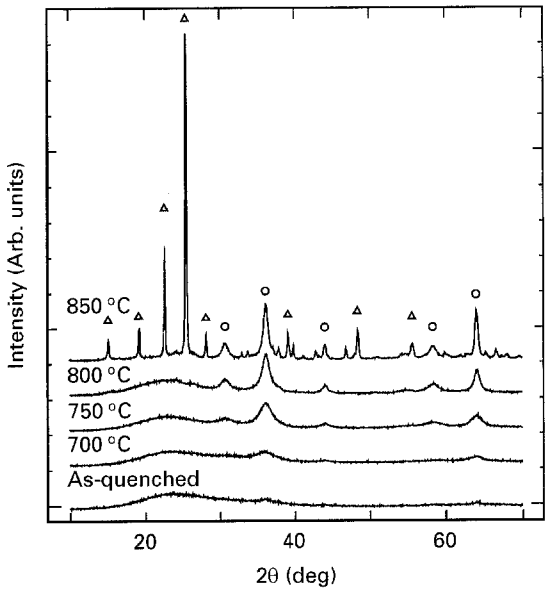

Figure 2 X-ray diffraction patterns of as-quenched and heat-treated specimens. The temperature indicated in the figure represents the heat-treatment temperature. (○, △) denote the diffraction lines attributed to $LiGa_5O_8$ and $LiGaSi_2O_6$, respectively.

1 mm thick, and heat-treated at 650–850 °C for 2 h in air to obtain glass-ceramics. For the measurements of temperature variation of the zero-phonon line (*R*-line), the as-quenched specimen was heat-treated at 800 °C for 2 h after heat treatment at 680 °C for 12 h.

$LiGa_5O_8:Cr^{3+}$ polycrystal was prepared by using the conventional solid-state reaction for comparison with the glass-ceramics. The molar ratio of chromium to lithium was 0.01. Raw materials of Li_2CO_3, Ga_2O_3 and Cr_2O_3 were mixed thoroughly and calcined at 1300 °C for 1 h. After the calcination was repeated three times, the powders were pressed under hydrostatic pressure and sintered at 1400 °C for 3 h.

2.2. Measurements

X-ray diffraction (XRD) measurements were carried out using CuK_α radiation to identify crystalline phases in the glass-ceramics and polycrystal.

Optical absorption spectra were measured using a spectrophotometer (Hitachi-330) at room temperature. Fluorescence spectra were measured using a fluorescence spectrophotometer (Hitachi-850). The excitation was carried out with a DCM dye laser (Spectra Physics Model 375) pumped by an argon ion laser (Coherent Innova 70). The measurements were carried out at room temperature to 8 K. For the measurements below room temperature, the specimen was cooled using a cryogenic refrigerator (Iwatani Plantech Model CRT-006-1000) and a compressor (Iwatani Plantech Model CA101). With the present equipment, low-temperatures down to 8 K can be obtained by utilizing the adiabatic expansion of helium gas supplied from the compressor.

Fluorescence lifetime measurements were performed as follows. The excitation was carried out using a DCM dye laser (Spectra Physics PDL-3) pumped with a pulsed Nd:YAG laser (Spectra Physics GCR-11). The time dependence of the fluorescence intensity was analysed with a monochromator (Ritsu MC-25NP) equipped with a photomultiplier (Hamamatsu Photonics R955) and a box car integrator (Stanford Research Systems SR250). The measurements were carried out at room temperature.

3. Results

Fig. 2 shows XRD patterns of as-quenched and heat-treated specimens. The temperature indicated in the figure denotes the heat-treatment temperature. In the specimens heat-treated below 800 °C, only $LiGa_5O_8$ crystal precipitated. For the specimen heat-treated at 850 °C, diffraction peaks of $LiGaSi_2O_6$ are observed in addition to those of $LiGa_5O_8$. These facts suggest that the exothermic peak at the lower temperature in the DTA curve (Fig. 1) is caused by the precipitation of $LiGa_5O_8$ and the peak at the higher temperature is ascribed to the precipitation of $LiGaSi_2O_6$. A very weak diffraction line found at about $2\theta = 36°$ in the XRD pattern of the as-quenched specimen is attributable to $LiGa_5O_8$ microcrystals which precipitated during the melt-cooling process. Fig. 3 shows the variation of average crystallite size of $LiGa_5O_8$ with

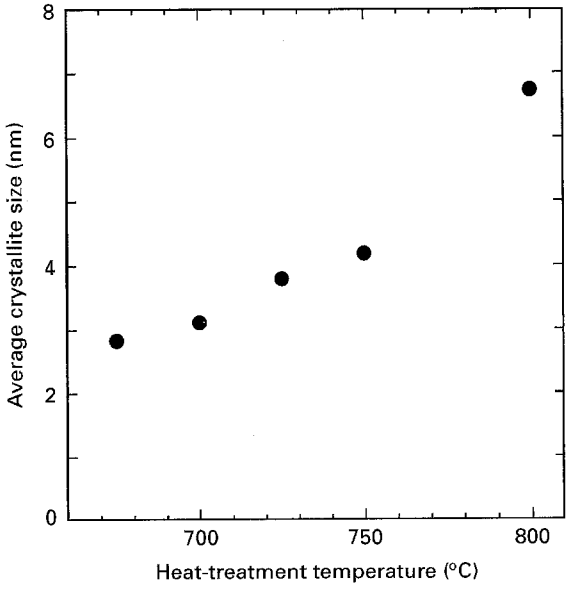

Figure 3 Variation of average crystallite size of $LiGa_5O_8$ with heat-treatment temperature.

heat-treatment temperature. The crystallite size was evaluated from the full-width at half-maximum of the XRD lines by using Scherrer's equation. As the heat-treatment temperature increases from 675 °C to 800 °C, the crystallite size increases from 3 nm to 7 nm.

Optical absorption spectra of the as-quenched and heat-treated specimens are shown in Fig. 4. It is obvious that the absorption peak positions for the heat-treated specimens are different from those for the as-quenched specimen. The absorption peaks around 16 000–17 000 cm^{-1} and 23 000–24 000 cm^{-1} correspond to the $^4A_2 \rightarrow {}^4T_2$ and $^4A_2 \rightarrow {}^4T_1$ transitions, respectively.

Room-temperature fluorescence spectra of the as-quenched and heat-treated specimens are shown in Fig. 5. The spectrum of the as-quenched specimen is shown by (a). (b)–(d) correspond to the heat-treatment temperatures, 700, 750 and 800 °C, respectively. The fluorescence intensity of the specimen heat treated at 800 °C is significantly high compared with that of the as-quenched specimen. Fig. 6 shows room temperature fluorescence spectra of $LiGa_5O_8:Cr^{3+}$ polycrystal and glass-ceramics heat-treated at 800 °C. The symbols PC and GC in the figure represent the polycrystal and transparent glass-ceramics, respectively. The fluorescence spectrum of the glass-ceramics resembles that of the polycrystal. This suggests that the Cr^{3+} ions are present in the $LiGa_5O_8$ microcrystals in the glass-ceramics. The fact that Cr^{3+} ions are effectively incorporated in the $LiGa_5O_8$ microcrystalline phase, while Co^{2+} ions are apt to remain in the glass matrix in the $LiGa_5O_8$-based transparent glass-ceramics [10], supports the idea that Cr_2O_3 acts as a nucleating agent. The fluorescence spectra measured

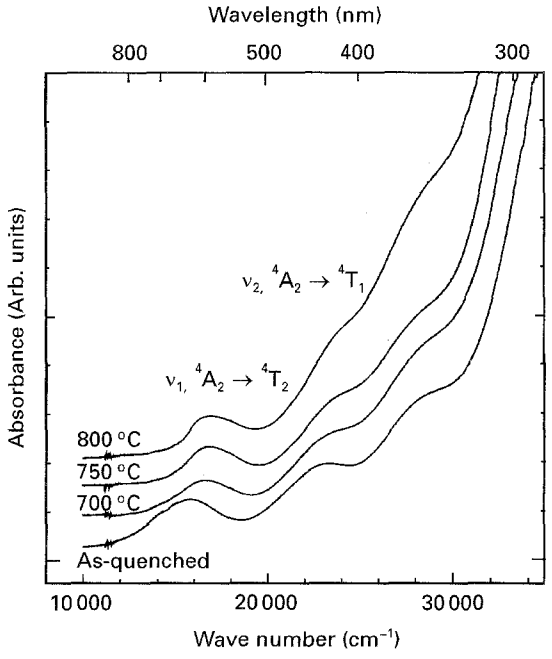

Figure 4 Optical absorption spectra of as-quenched and heat-treated specimens. The temperature indicated in the figure represents the heat-treatment temperature. Measurements were carried out at room temperature. The assignments of the absorption peaks are presented in the figure.

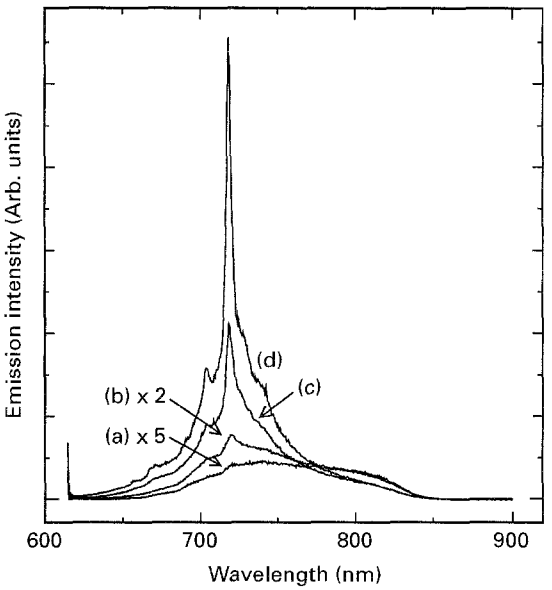

Figure 5 Room-temperature fluorescence spectra of (a) the as-quenched specimen, and the specimens heat-treated at (b) 700 °C, (c) 750 °C and (d) 800 °C. The excitation was carried out with an argon ion laser-pumped DCM dye laser at wavelength of 614 nm.

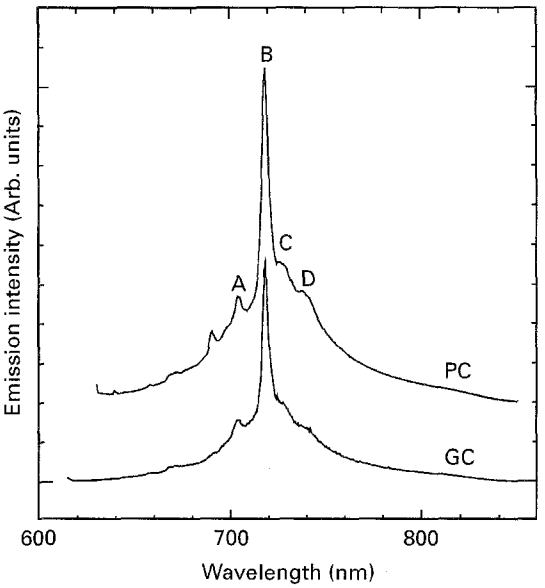

Figure 6 Room-temperature fluorescence spectra of glass-ceramics heat-treated at 800 °C and $LiGa_5O_8:Cr^{3+}$ polycrystal. GC and PC denote the glass-ceramics containing $LiGa_5O_8:Cr^{3+}$ and polycrystalline $LiGa_5O_8:Cr^{3+}$, respectively. The excitation was carried out with an argon ion laser-pumped DCM dye laser at a wavelength of 614 nm. The assignments of peaks labelled A–D are presented in the text.

at room temperature (RT) and 8 K for the specimen heat-treated at 800 °C are shown in Fig. 7. The peak labelled B in Figs 6 and 7 is the zero-phonon line. The peaks labelled as A, C and D in these figures are attributable to the vibronic transitions or Cr^{3+}–Cr^{3+} interactions. This is discussed in the following section.

The time dependence of the fluorescence intensity measured at room temperature for the specimens heat treated at 700 and 800 °C is shown in Fig. 8. The excitation and fluorescence wavelengths are 625 and 717 nm, respectively. Fig. 9 shows the time dependence of fluorescence intensity for the specimen heat treated at 800 °C. The fluorescence wavelengths are 717 and 770 nm. The former wavelength corresponds

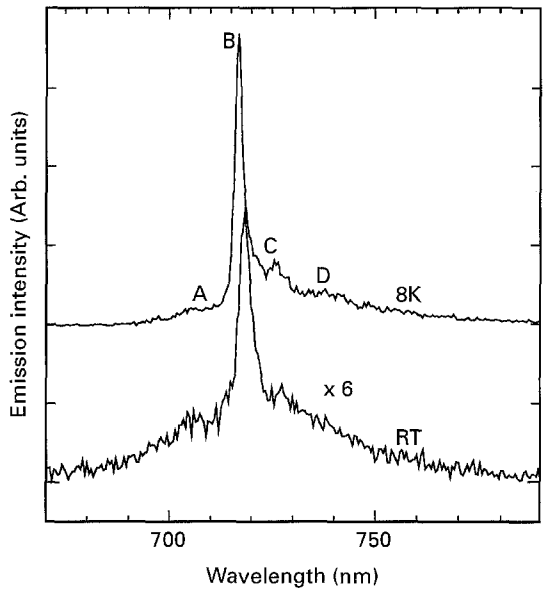

Figure 7 Fluorescence spectra of the specimen heat-treated at 800 °C measured at room temperature (RT) and 8 K. The assignments of peaks A–D are presented in the text.

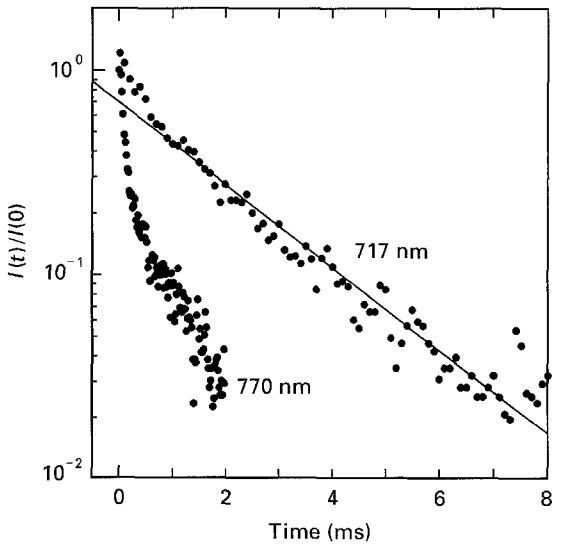

Figure 9 Time dependence of the fluorescence intensity for the specimen heat-treated at 800 °C. The fluorescence wavelength is indicated in the figure. The excitation source is a DCM dye laser pumped with a pulsed Nd:YAG laser. The excitation wavelength is 625 nm. The measurements were performed at room temperature.

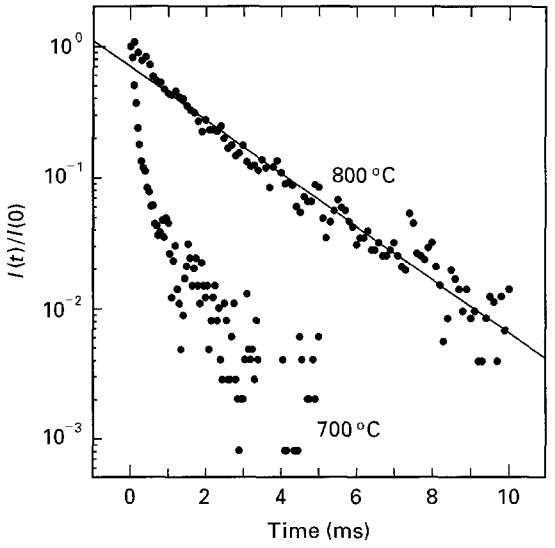

Figure 8 Time dependence of the fluorescence intensity for specimens heat-treated at 700 and 800 °C. (——) A single exponential decay curve, which gives the lifetime of 2 ms for the specimen heat treated at 800 °C. The excitation source is a DCM dye laser pumped with a pulsed Nd:YAG laser. The excitation wavelength is 625 nm. The measurements were performed at room temperature.

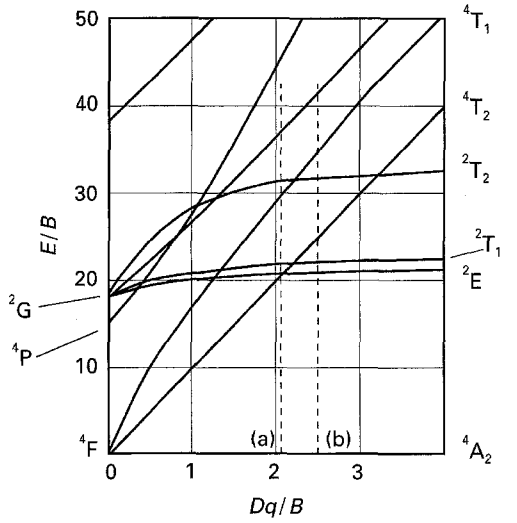

Figure 10 The Tanabe–Sugano diagram for Cr^{3+} in the octahedral site. The values of Dq/B are given for (a) the as-quenched specimen and (b) glass-ceramics heat-treated at 800 °C.

to the most intense fluorescence peak in Figs 5–7 (peak B in Figs 6 and 7). The latter wavelength lies near the broad emission band observed for the as-quenched specimen as shown in Fig. 5. The decay is more rapid for the fluorescence at 770 nm.

4. Discussion

The Cr^{3+} ion occupies more preferentially the octahedral site than the tetrahedral site in glasses and crystals because three 3d electrons of Cr^{3+} can take lower t_{2g} level in the octahedral site. The Tanabe–Sugano diagram for the Cr^{3+} in the octahedral site is shown in Fig. 10. In the absorption spectra of the present specimens (see Fig. 4), the lowest-energy and middle-energy peaks, the energies of which are indicated by ν_1 and ν_2, respectively, are attributed to the $^4A_2 \rightarrow {}^4T_2$ and $^4A_2 \rightarrow {}^4T_1$ (F) transitions, respectively. The absorption peak due to the $^4A_2 \rightarrow {}^4T_1$ (P) transition is barely observed because it is hidden by the absorption edge. The position of the peak around 27 800 cm^{-1} for the heat-treated specimens is not different from that for the as-quenched specimen. This suggests that the origin of this peak is not identical with the origin of the two lower-energy peaks. This peak is attributable to the charge transfer of the Cr^{6+} ion [12, 13]. The energies of the absorption peaks are related to the ligand field parameters, Dq and B, as follows [14]

$$\nu_1 = 10Dq \tag{1}$$

$$\nu_2 = 7.5B + 15Dq - \frac{1}{2}(225B^2 + 100Dq^2 - 10BDq)^{1/2} \tag{2}$$

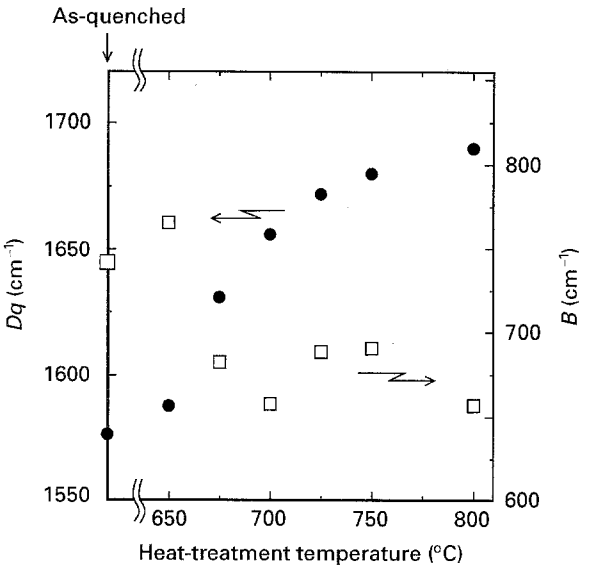

Figure 11 Heat-treatment temperature dependence of the ligand field parameters (●) Dq and (□) B. The values of the as-quenched specimen are also shown.

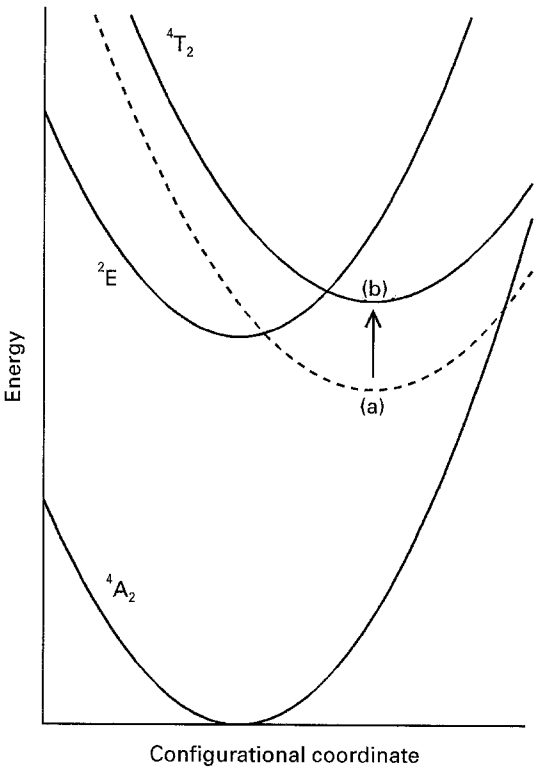

Figure 12 Energy level diagram for Cr^{3+} in (a) glass and (b) glass-ceramics, schematically illustrated using the configurational coordinate model.

Dq for the present specimens was calculated using Equation 1 and is shown in Fig. 11. Dq increases with an increase in the heat-treatment temperature: Dq of a specimen heat-treated at 800 °C is 1690 cm^{-1}. This value is smaller than Dq for the Cr^{3+} in $ZnAl_2O_4$ microcrystal precipitated in transparent glass-ceramics, i.e. about 1850 cm^{-1} [9]. This reflects the smaller ionic radius of Ga^{3+} compared with Al^{3+}. The Racah parameter, B, was calculated using Equations 1 and 2. The variation of B with heat-treatment temperature is also shown in Fig. 11. When the size of the crystallite is large, the scattering of incident light by crystallites causes a reduction of transmission. As the result, a very intense absorption appears in the ultraviolet region. Actually, it is found from Figs 3 and 4 that the transmission of the ultraviolet region decreases as the size of the crystallite increases. This makes it difficult to determine the energy of the $^4A_2 \rightarrow {}^4T_1$ transition accurately, leading to uncertainty in B values. The B values shown in Fig. 11 are scattered for this reason. Nonetheless, it is obvious that the B value tends to decrease with an increase in the heat-treatment temperature. These variations of Dq and B result in an increase in Dq/B with an increase in the heat-treatment temperature. The values of Dq/B for the as-quenched specimen and specimen heat-treated at 800 °C are presented in Fig. 10a and b, respectively. Dq/B changes from 2.1 to 2.5 when the matrix for the Cr^{3+} ion is transferred from glass to $LiGa_5O_8$ crystallite. Fig. 12 shows the configurational coordinate model for the ^2E and $^4T_2$ levels. The difference in the energy level between glass and glass-ceramics is schematically illustrated. Fig. 12a and b represent the $^4T_2$ level for the glass and glass-ceramics, respectively. The lowest energy level among the excited levels is $^4T_2$ for the Cr^{3+} in the glass and ^2E for the Cr^{3+} in the glass-ceramics.

In Figs 5–7, the intense fluorescence peak around 717 nm is attributed to the zero-phonon line in the $^2E \rightarrow {}^4A_2$ transition for the Cr^{3+} in $LiGa_5O_8$ crystal, i.e. R-line [15–17]. The fluorescence peak around 705 nm (peak A in Figs 6 and 7) is very weak when the measurement temperature is low. It is thought that peak A is ascribed to the R_2-line or hot band of the R_1-line. Glynn *et al.* assigned this peak to a resonance between them [15]. The peak labelled C is attributable to Cr^{3+}–Cr^{3+} pair interaction, as suggested by MacCraith *et al.* [16]. Peak D is assigned to a phonon sideband according to Szymczak *et al.* [17]. On the other hand, the broad band around 750 nm in the fluorescence spectra of the specimens heat-treated at low elevated temperatures, as well as the as-quenched specimen, is attributed to $^4T_2 \rightarrow {}^4A_2$ transition. The broadness of this band comes from the fact that this band is due to the vibronic transition (see Fig. 12).

In the fluorescence decay curves for the specimen heat-treated at 800 °C, shown in Fig. 9, the fluorescences at 717 and 770 nm correspond to transitions from ^2E and $^4T_2$, respectively. The lifetime of ^2E is about ten times longer than that of $^4T_2$; the lifetime of ^2E was approximately evaluated to be 2 ms by assuming the time dependence of the logarithm of the fluorescence intensity to be linear. This value is comparable to the lifetime for the R-line in ruby at room temperature, i.e. 3 ms [18]. The time dependence of the fluorescence intensity for the glass-ceramics heat-treated at 700 °C is not expressed by a single exponential curve (see Fig. 8). This presumably comes from the fact that the overlap of $^4T_2$ and ^2E states occurs because the difference in energy between these states is not so large in this case. Namely, the ligand field strength around Cr^{3+} is not so high in the specimen heat-treated at 700 °C as in the specimen heat-treated at 800 °C. This is coincident with the Dq values shown in Fig. 11.

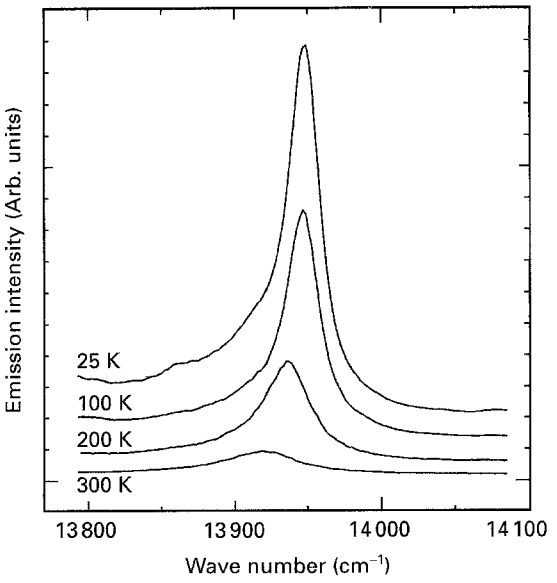

Figure 13 Fluorescence spectra at various temperatures for the $LiGa_5O_8:Cr^{3+}$-containing glass-ceramics heat-treated at 680 °C for 12 h and reheated at 800 °C for 2 h.

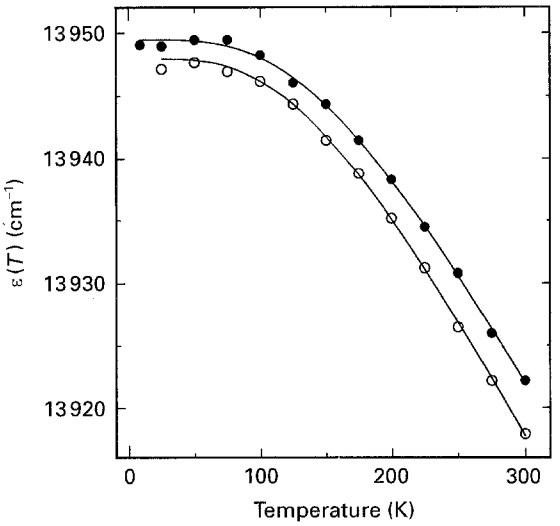

Figure 14 Temperature dependence of the peak position of the R-line. (●) $LiGa_5O_8:Cr^{3+}$ polycrystal and (○) glass-ceramics heat treated at 680 °C for 12 h and reheated at 800 °C for 2 h. (——) The temperature dependence was calculated assuming the Raman process for the electronic transition and the Debye model for the vibrational density of state.

The position of the fluorescence peak labelled B in Fig. 7 shifts to a lower wave number as the measurement temperature increases. Fig. 13 shows fluorescence spectra at various temperatures for the specimen heat-treated at 680 °C for 12 h and reheated at 800 °C for 2 h, which contains $LiGa_5O_8:Cr^{3+}$ crystallites of about 12 nm. The peak position of the R-line shifts to a lower wave number with an increase in temperature. McCumber and Sturge [19] investigated the temperature dependence of linewidth and peak position of the R-lines in ruby. They revealed that the temperature dependence was describable in terms of the Raman process as the electronic transition. In the case of the Raman process, the temperature dependence of the peak position is expressed by the following equations when the Debye model is assumed for the vibrational density of state [19]

$$\varepsilon(T) = \varepsilon(0) + \alpha\left(\frac{T}{T_D}\right)^4 \int_0^{T_D/T} \frac{x^3}{e^x - 1}\,dx \qquad (3)$$

$$\alpha = \frac{3\hbar\omega_D^4}{2\pi^2\rho v^5}\left(\langle i|V^{(2)}|i\rangle + \sum_{m\neq i}\frac{|\langle i|V^{(1)}|m\rangle|^2}{W_i - W_m}\right) \qquad (4)$$

where $\varepsilon(0)$ is the peak position at 0 K, T_D is the Debye temperature, ω_D is the Debye wave number, ρ is the density, v is the sound velocity, $V^{(n)}$ s are the orbital operators for the impurity d electrons, W_i is the energy of the initial state, and W_m is the energy of the middle state. The measurement temperature dependence of the peak position is shown in Fig. 14. The open and closed circles denote the transparent glass-ceramics and polycrystalline $LiGa_5O_8:Cr^{3+}$, respectively. The solid curves are calculated ones drawn by using Equation 3 under the assumption that α is independent of temperature. As Fig. 14 shows, in the present $LiGa_5O_8:Cr^{3+}$ system, the temperature variation of the peak position of the R-line is describable in terms of the Raman process with the Debye model. The three parameters $\varepsilon(0)$, α and T_D obtained from this analysis are shown in Table I. Considering the resolving power of the fluorescence spectrophotometer used in the present experiment, the error in the fluorescence peak position is about 1 cm^{-1}, leading to an error of a few tens of kelvin in the Debye temperature. Nonetheless, it can be said that the Debye temperature for the glass-ceramics is lower than that for the polycrystal. This supports the view that softening of phonons occurs in microcrystals.

TABLE I Peak position at 0 K, $\varepsilon(0)$, parameter α expressed by Equation 4, and Debye temperature, T_D, evaluated from the analysis of the temperature dependence of the peak position of the R-line for transparent glass-ceramics and $LiGa_5O_8:Cr^{3+}$ polycrystal

Specimen	$\varepsilon(0)$ (cm^{-1})	α (cm^{-1})	T_D (K)
Glass-ceramics	13948	−430	610
Polycrystal	13950	−450	660

5. Conclusion

Transparent glass-ceramics containing $LiGa_5O_8:Cr^{3+}$ crystallites were successfully prepared by the heat treatment of glassy as-quenched material with the composition $13Li_2O \cdot 23Ga_2O_3 \cdot 64SiO_2 \cdot 0.1Cr_2O_3$. The average crystallite size is about 3–7 nm as evaluated from the full-width at half-maximum of the X-ray diffraction lines. The ligand field strength of Cr^{3+} is higher in the transparent glass-ceramics, i.e. in the $LiGa_5O_8$ microcrystal, than in the glass. Consequently, the fluorescence due to the $^2E \rightarrow {}^4A_2$ transition is predominant in the fluorescence spectrum of transparent glass-ceramics, in particular, in the specimen heat-treated at higher temperatures. The lifetime of the ^2E level is 2 ms for the specimen heat-treated at 800 °C. This value is comparable to the

lifetime for R-lines in the ruby. The temperature dependence of the peak position of the R-line for the present transparent glass-ceramics is describable in terms of the Raman process with the Debye model. The softening of phonons was demonstrated for the $LiGa_5O_8:Cr^{3+}$ microcrystal precipitated in the transparent glass-ceramics.

Acknowledgement

This work was financially supported by a Grant-in-Aid for Encouragement of Young Scientists (05750747).

References

1. R. REISFELD, *Mater. Sci. Eng.* **71** (1985) 375.
2. R. REISFELD, A. KISILEV, A. BUCH and M. ISH-SHALOM, *J. Non-Cryst. Solids* **91** (1987) 333.
3. A. KISILEV, R. REISFELD, A. BUCH and M. ISH-SHALOM, *Chem. Phys. Lett.* **129** (1986) 450.
4. F. DURVILLE, B. CHAMPAGNON, E. DUVAL, G. BOULON, F. GAUME, A. F. WRIGHT and A. N. FITCH, *Phys. Chem. Glasses* **25** (1984) 126.
5. F. DURVILLE, B. CHAMPAGNON, E. DUVAL and G. BOULON, *J. Phys. Chem. Solids* **46** (1985) 701.
6. W. NIE, G. BOULON, C. MAI, C. ESNOUF, R. XU and J. ZARZYCKI, *J. Non-Cryst. Solids* **121** (1990) 282.
7. X. F. LIU, J. M. PARKER, E. A. HARRIS and C. TOPACLI, in "The Physics of Non-Crystalline Solids", edited by L. D. Pye, W. C. LaCourse and H. J. Stevens (Taylor and Francis, London, 1992) p. 642.
8. K. TANAKA, K. HIRAO, T. ISHIHARA and N. SOGA, *J. Ceram. Soc. Jpn* **101** (1993) 102.
9. T. ISHIHARA, K. TANAKA, K. HIRAO and N. SOGA, *J. Soc. Mater. Sci. Jpn* **42** (1993) 484.
10. K. TANAKA, T. MUKAI, T. ISHIHARA, K. HIRAO, N. SOGA, S. SOGO, M. ASHIDA and R. KATO, *J. Am. Ceram. Soc.* **76** (1993) 2839.
11. T. ISHIHARA, K. TANAKA, K. HIRAO and N. SOGA, *Bull. Chem. Soc. Jpn* **67** (1994) 993.
12. A. PAUL and R. W. DOUGLAS, *Phys. Chem. Glasses* **8** (1967) 151.
13. L. J. ANDREWS, A. LEMPICKI and B. C. McCOLLUM, *J. Chem. Phys.* **74** (1981) 5526.
14. J. E. HUHEEY, E. A. KEITER and R. L. KEITER, "Inorganic Chemistry", (Harper Collins College, New York, 1993) p. 447.
15. T. J. GLYNN, J. P. LARKIN, G. F. IMBUSCH, D. L. WOOD and J. P. REMEIKA, *Phys. Lett. A* **30** (1969) 189.
16. B. D. MacCRAITH, T. J. GLYNN, G. F. IMBUSCH, J. P. REMEIKA and D. L. WOOD, *Phys. Rev. B* **25** (1982) 3572.
17. H. SZYMCZAK, M. WARDZYŃSKA and I. E. MYLNIKOVA, *J. Phys. C* **8** (1975) 3937.
18. V. UROŠVIĆ, B. PANIĆ, B. JOVANIĆ and Lj. ZEKOVIĆ, *Chem. Phys. Lett.* **155** (1989) 325.
19. D. E. McCUMBER and M. D. STURGE, *J. Appl. Phys.* **34** (1963) 1682.

Received 1 December 1994
and accepted 1 December 1995